Analyst

PAPER

View Article Online
View Journal | View Issue

Cite this: *Analyst*, 2016, **141**, 6557

Design of luciferase-displaying protein nanoparticles for use as highly sensitive immunoassay detection probes

Yusuke Ikeda, Yasumasa Mashimo, Masayasu Mie and Eiry Kobatake*

Received 1st June 2016,
Accepted 1st November 2016

DOI: 10.1039/c6an01253a

www.rsc.org/analyst

In this study, we developed a protein nanoparticle-based immunoassay to detect cancer biomarkers using a bioluminescent fusion protein. This method relies on the use of protein nanoparticles comprised of genetically-engineered elastin-like polypeptides (ELPs) fused with poly-aspartic acid tails (ELP-D), previously developed in our lab. The sizes of the self-assembled ELP-D nanoparticles can be regulated at the nanoscale by charged repulsion of the poly-aspartic acid chains. To improve the sensitivity of enzyme-linked immunosorbent assays (ELISAs), we herein demonstrate the multivalent display of NanoLuc® (Nluc) luciferase and a biotin acceptor peptide (BAP) on the surfaces of ELP-D nanoparticles, and demonstrate the sensitivity of these multivalent nanoparticles as detection probes. The fusion protein comprised of ELP-D and Nluc-BAP (ELP-D-Nluc-BAP) was found to form nanoparticles with Nluc and BAP displayed multivalently on their surfaces. Moreover, the use of the nanoparticles in ELISA resulted in a detection sensitivity for α-fetoprotein (AFP) about 10 times higher than that of an assay relying on the use of the monomeric version of the fusion protein. Taken together, ELP-D-based nanoparticles displaying multivalent luciferases on their surfaces enable the construction of an ELISA with enhanced sensitivity.

Introduction

Enzyme-linked immunosorbent assays (ELISAs) have proven to be indispensable methods for the sensitive and selective determination of trace substances in various fields (*e.g.*, clinical, diagnostic, food, environmental, *etc.*). In particular, clinical biomarkers require highly-sensitive detection methods because early diagnosis of disease is important for effective treatment.[1–4] To improve the detection sensitivity of such biomarkers, various techniques have been employed to enhance conventional ELISA methods.

One of the most popular strategies is the use of enzyme-functionalized carriers as tracers to improve ELISA sensitivity by loading large amounts of enzymes onto individual sandwich immunological reaction events.[5,6] The number of enzymes displayed on the carrier determines the amplification of the signal. For example, Ambrosi *et al.* demonstrated the use of gold nanoparticles (AuNPs) as multi-enzyme carriers in an ELISA for the detection of CA15-3 antigen in blood samples.[7] The AuNP-based amplification platforms were found to dramatically enhance the intensity of the immunological reaction event signal, leading to ultrasensitive bioassays.

Recently, several nanomaterials have been used to amplify the detection signal in biosensors. These nanomaterials include gold nanoparticles,[8–10] quantum dots,[11,12] carbon nanotubes,[13–15] carbon nanospheres,[16] graphene oxide[17,18] and silica nanoparticles.[19,20] For example, Xu *et al.* developed a graphene-based signal-amplification nanoprobe by combining anti-immunoglobulin G (anti-IgG) and horseradish peroxidase (HRP) with graphene oxide (GO).[21] Yu *et al.* demonstrated the construction of electrochemical immunosensors using single-wall carbon nanotubes with multi-label antibodies for highly-sensitive detection of prostate specific antigen (PSA).[22] Wu *et al.* developed an ultrasensitive immunosensor for the detection of α-fetoprotein (AFP), based on an HRP-functionalized SiO_2 label.[23] These approaches provided detection limits that were much more sensitive than conventional methods; the nanomaterials, therefore, exhibit the potential to become universal probes for diagnostics. However, such materials often do not satisfy the requirements needed for the design of carriers that can display multivalent enzymes, owing to inherent surface area limitations. Moreover, uniformly-sized nanostructures are often not obtained and become instable after surface biological functionalization, resulting in quantitative insufficiency. Therefore, the design of functional

Department of Life Science and Technology, School of Life Science and Technology, Tokyo Institute of Technology, 4259 Nagatsuta, Midori-ku, Yokohama 226-8502, Japan. E-mail: ekobatak@bio.titech.ac.jp; Fax: +81 45 924 5779; Tel: +81 45 924 5760

nanoprobes for use as highly sensitive biosensors remains challenging.

Herein, we designed elastin-like polypeptide (ELP)-based protein nanoparticles displaying multivalent enzymes. ELPs are well-known recombinant proteins widely used as thermo-responsive materials.[24,25] In previous studies, we developed protein nanoparticles comprised of ELPs fused with poly-aspartic acid chains (ELP-D). Above the transition temperature, ELP-D forms aggregates whose sizes are regulated to around 30 nm as a result of the charge repulsion of the poly-aspartic acid chains.[26] Moreover, nanoparticles formed from genetically modified ELP-D enable the display of multivalent proteins on their surfaces, without the need for chemical modification. For example, ELP-based nanoparticles displaying multivalent epidermal growth factor (EGF) were genetically designed to target tumor cells overexpressing the EGF receptor.[27] Thus, ELP-D based protein nanoparticles exhibit the ability to be used as carriers displaying multivalent enzymes.

In this study, we developed an enhanced ELISA using protein nanoparticles displaying multivalent enzymes as detection probes of α-fetoprotein (AFP). The design of the enhanced ELISA, which relies on the use of protein nanoparticles, is illustrated in Fig. 1. NanoLuc® luciferase (Nluc) was fused to ELP-D and used as the signal-generating enzyme, while a biotin acceptor peptide (BAP) was fused to the end of the fusion protein for modification with biotin in *E. coli*. The resultant fusion protein, ELP-D-Nluc-BAP, was found to form nanoparticles upon heating above the transition temperature. The nanoparticles were subjected to an ELISA using biotin-labeled secondary antibodies for the binding of protein nanoparticles *via* biotin–streptavidin binding. Signal intensities were increased due to the presence of more enzyme molecules catalyzing the substrate. Finally, we demonstrated the utility of this system using human AFP as a test analyte.

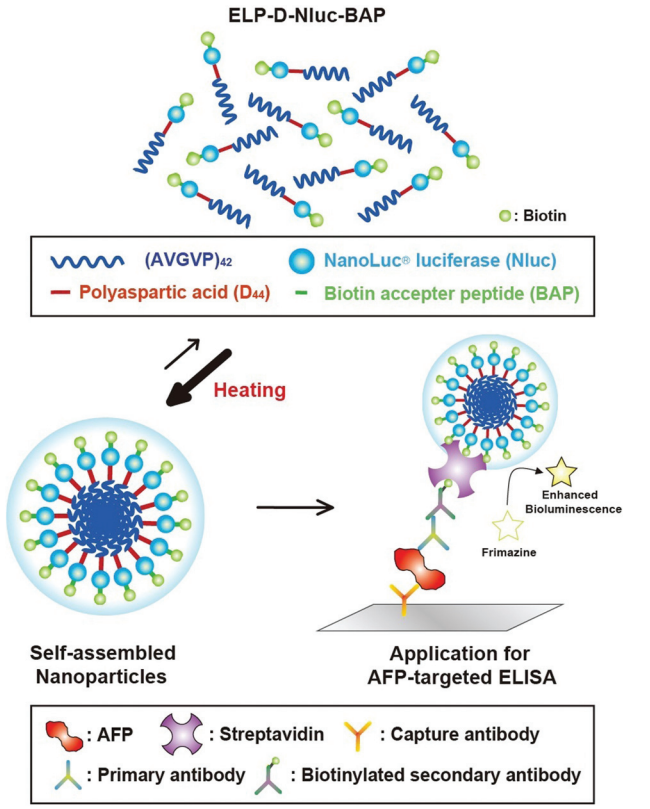

Fig. 1 Schematic of preparation of ELP-D nanoparticle probes and the ELP-D nanoparticle probe-based ELISA procedure. ELP with a poly-aspartic acid chain, Nluc and BAP exist as a monomeric protein below the transition temperature, and forms nanoparticles above the specific temperature. Then, the nanoparticle-based probes can be stored ready for use. For assays, AFP was immobilized on the microplate which is coated by mouse anti-human AFP IgG. Primary and biotin-labeled secondary antibodies were added stepwise and bound to AFP. Nanoparticle probes were captured by a secondary antibody *via* streptavidin. Finally, a substrate solution was added and reacted with Nluc on probes.

Experimental

Materials

Restriction enzymes and ligase were purchased from Takara Bio (Shiga, Japan). *Escherichia coli* JM109 and BLR (DE3) were purchased from Takara Bio (Shiga, Japan) and Novagen (Madison, WI), respectively. The pNL1.1 [Nluc] vector was purchased from Promega (Madison, WI). Human α-fetoprotein (AFP) was purchased from Fitzgerald Industries International (Acton, MA). Antibodies used in the ELISA experiments were all purchased from Funakoshi (Tokyo, Japan). All other chemicals were of analytical grade.

Construction of plasmids

For the construction of pET28b-$(PAVGV)_{42}$-D_{44}-Nluc-BAP-CHis, a structural gene of NanoLuc® (Nluc) luciferase was amplified from the pNL1.1[Nluc] vector by PCR using a pair of primers, namely 5′-GGGGAATTCGCCATGGGCGTCGACATGGTCTTCACA CTCGAAGATTTC-3′, containing *Eco*R I, *Nco* I and *Sal* I restriction enzyme sites, and 5′-TCAGAATTCCTCGAGCGCCAGAATGCGTT CGCACAGCCG-3′, containing *Xho* I and *Eco*R I restriction enzyme sites, and inserted into pUC18 digested with *Sma* I followed by sequencing. The resulting plasmid, pUC-Nluc, was digested with *Nco* I and *Eco*R I. The obtained Nluc gene fragment was inserted into pET28b-BAP-CHis constructed in our laboratory. The resulting plasmid, pET28b-Nluc-BAP-CHis, was digested with *Nco* I and *Sal* I for insertion of the $(PAVGV)_{42}$-D_{44} gene fragment derived from pET28b-$(PAVGV)_{42}$-D_{44}-CHis, previously constructed in our lab, and digested with *Nco* I and *Xho* I. The resulting plasmid was named pET28b-$(PAVGV)_{42}$-D_{44}-Nluc-BAP-CHis.

Expression and purification of fusion proteins

The plasmids pET28b-$(PAVGV)_{42}$-D_{44}-CHis and pET28b-$(PAVGV)_{42}$-D_{44}-Nluc-BAP-CHis were transfected into *E. coli* BLR (DE3) competent cells *via* heat-shock. Transformed cells were inoculated in LB media supplemented with 0.1 mg mL^{-1} kanamycin and incubated at 37 °C. Protein expression was induced by addition of isopropyl-β-D-thiogalactopyranoside (IPTG) at a concentration of 0.5 mM and D-biotin at 50 μM when an

optical density of 0.6 at 660 nm was reached. After overnight induction at 25 °C, cells were harvested by centrifugation at 8000*g* for 3 min at 4 °C. The cell pellet was resuspended in phosphate buffered saline (PBS) and disrupted by sonication. The cell lysates were centrifuged at 17 000*g* for 15 min at 4 °C to remove insoluble cellular debris. Next, the collected fractions were applied to TALON Metal Affinity Resins (Clontech) to purify the proteins using a His-tag. After 1 h incubation, the columns were washed 5 times with 3 column volumes of wash buffer (20 mM Na_2HPO_4, 500 mM NaCl), followed by 5 washes with 3 volumes of the same buffer including 10 mM imidazole. The same volume of elution buffer (20 mM Na_2HPO_4, 500 mM NaCl, 100 mM imidazole) was then added to elute the fusion proteins. The purified proteins, $(PAVGV)_{42}$-D_{44}-Nluc-BAP (ELP-D-Nluc-BAP) and $(PAVGV)_{42}$-D_{44} (ELP-D), were dialyzed against PBS using a Slide-A-lyzer dialysis cassette (Pierce, 10 000 MW, 0.5–3.0 ml) and analyzed by SDS-PAGE (12% acrylamide gels). Concentrations of the purified proteins were determined using the BCA assay kit (Pierce).

Western blotting of biotinylated fusion protein

SDS-PAGE (12% acrylamide) was performed under denaturing conditions in the presence of β-mercaptoethanol. Proteins were transferred electrophoretically to a polyvinylidene fluoride (PVDF) membrane (Immobilon transfer membrane, Millipore) for western blotting. Membranes were blocked with Blocking One (Nacalai Tesque, Inc., Japan) for 0.5 h followed by incubation with alkaline phosphatase (ALP)-labeled streptavidin (Sigma-Aldrich) for another 10 min. After washing 3 times with PBS-T buffer (PBS with 0.05% Tween 20), the ALP activity was detected using Fast Red TR/Naphthol AS-MX tablets (Sigma-Aldrich).

Thermostability of Nluc fused to ELP

ELP-D-Nluc-BAP fusion proteins were incubated at specific temperatures (4, 25, 30, 35, 40, 45, 50, 55, 60, 65, 70, 75, 80 °C) for 20 min. After incubation, 50 μL of ELP-D-Nluc-BAP (1 pM) were added to equal amounts of Nano-Glo® Luciferase Assay Reagent (Promega). Bioluminescence was measured using a luminometer (LMax384, Molecular Devices) with a 96-well white polystyrene plate (Costar #3912, Corning Incorporated).

Thermal characterization and dynamic light scattering

The transition temperatures of the purified proteins and nanoparticle sizes were evaluated as previously described.[27] Briefly, purified proteins were filtered using a 0.22 μm filter, and dissolved in PBS (pH 7.4) at a final concentration of 0.5 mg mL^{-1}. Turbidity was evaluated using a UV-vis spectrometer (DU-7500, Beckman Coulter) at 350 nm. The sample was heated from 20 to 50 °C, and subsequently cooled to 20 °C using a temperature gradient of 1 °C min^{-1}. Light scattering data were measured by a Nano-ZS (Sysmex). Samples were equilibrated at the measuring temperature for 10 min prior to data collection. Light scattering data at 90° and 633 nm were collected for at least 10 s × 10 runs. The sizes of the proteins were calculated based on the assumption that the viscosity of PBS was the same as that of water. The particle sizes with a single-peaked distribution were calculated by the Cumulant method. Conversion from an intensity distribution to a volume distribution was performed with the software connected to the Nano-ZS.

Protein nanoparticle-based ELISA for detection of AFP

A 96-well white polystyrene microtiter-plate (Costar #3922, Corning) was coated for 1 h at 37 °C with 100 nM of mouse monoclonal anti-human AFP antibody (Exbio, Vestec, Czech Republic) diluted with PBS (8.1 mM Na_2HPO_4, 2.7 mM KCl, 1.47 mM KH_2PO_4, 137 mM NaCl, pH 7.4). After washing 3 times with PBS-T (PBS with 0.05% Tween 20), the microtiter plate was blocked with Blocking One at 37 °C overnight. After washing with PBS-T, various concentrations of AFP (1–10 000 pg mL^{-1}) in 5% bovine serum albumin (BSA) or human blood serum (Sigma-Aldrich) were incubated in the wells for 1 h at 37 °C. After washing with PBS-T, rabbit polyclonal anti-human AFP IgG (Monosan, Netherlands) diluted with PBS was added and incubated for 1 h at 37 °C. After washing, biotin-labeled goat polyclonal anti-rabbit IgG (H + L) (Vector, USA) was added and incubated for 1 h at 37 °C. After washing with PBS-T, 1 μM of streptavidin (Wako, Japan) was added and incubated for 1 h at 37 °C. After washing with PBS-T, 200 nM of ELP protein diluted with PBS was added for blocking nonspecific binding of ELP-D-Nluc-BAP nanoparticles, and incubated for 1 h at 25 °C. After washing with PBS-T, 200 nM of ELP-D-Nluc-BAP nanoparticles formed by incubation at 45 °C for 20 min was added and incubated for 1 h at 25 °C. After washing, 30 μL of the Nano-Glo® Luciferase Assay Reagent was added and the bioluminescence signal was measured by a luminometer. Based on the standard deviation of the response and the slope on this result: the limit of detection (LOD) was calculated by IUPAC approach: 3.3 × standard deviation of low concentration/slope of the calibration line.

Results and discussion

Purification and characterization of ELP-D-Nluc-BAP fusion proteins

The design of the fusion proteins ELP-D and ELP-D-Nluc-BAP is shown in Fig. 2A. Here, poly(PAVGV) was employed as the ELP sequence, and was shown to form stable microparticles at the transition temperature. After incubation above the transition temperature, the reversible dissolution of the poly (PAVGV) suspension is strongly impeded, even after cooling to temperatures below the transition temperature, due to the lack of water molecules between the amide groups. Fusion of a poly-aspartic acid chain (D) with ELP allows the size of the resultant ELP aggregates to be regulated on the nanoscale by charged repulsion of the poly-aspartic acid chains.[27,28] Nluc was fused to ELP-D as the signal-generating enzyme. Nluc is an engineered luciferase derived from *Oplophorus gracilirostris* (19 kDa), which uses a coelenterazine derivative (furimazine) as its substrate for bioluminescence. Its small size and high

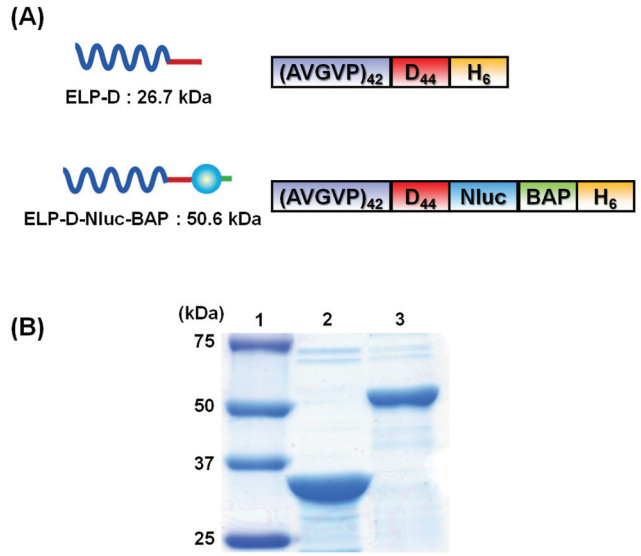

Fig. 2 Expression and purification of fusion proteins. Construction of fusion proteins (A). SDS-PAGE analysis (B) of purified ELP-D and ELP-D-Nluc-BAP proteins. Lane 1: molecular weight marker; lane 2: ELP-D; lane 3: ELP-D-Nluc-BAP.

physical stability makes it suitable for use as a signal enzyme when displayed on the surface of nanoparticles.[29] Nluc also exhibits the greatest thermostability (T_m = 60 °C) of all the luciferases, and, therefore, was expected to retain its bioluminescent activities even after heating and formation of nanoparticles. BAP, a small peptide of 15 amino acids in length, is a target for the biotin–protein ligase BirA. In *E. coli*, biotin is covalently conjugated to the single lysine residue of the BAP sequence by BirA.[30,31] Protein nanoparticles displaying BAP, therefore, exhibit the ability to bind to biotinylated antibodies *via* streptavidin. The fusion proteins ELP-D and ELP-D-Nluc-BAP were expressed in *E. coli* by addition of IPTG and purified by TALON Metal affinity chromatography. The sizes and purity of the fusion proteins were analyzed by 12% SDS-PAGE, and bands were observed for both ELP-D and ELP-D-Nluc-BAP (Fig. 2B). The ELP-D band appeared larger than the expected molecular mass (26.7 kDa), which has been previously reported to be due to the inherent physicochemical characteristics of ELPs.[32] The ELP-D-Nluc-BAP band, on the other hand, appeared at nearly the predicted molecular mass (50.6 kDa), suggesting that the presence of the Nluc sequence cancels-out the effects of the inherent physicochemical characteristics of ELPs.

Next, biotinylation of ELP-D-Nluc-BAP was evaluated by western blotting. ALP-modified streptavidin was used for detection of biotinylation. As shown in Fig. 3A, ELP-D did not show any bands, while ELP-D-Nluc-BAP showed a single band at the predicted molecular mass. These results demonstrate that the ELP-D-Nluc-BAP fusion protein was biotinylated and able to bind to streptavidin.

The thermostability of ELP-D-Nluc-BAP was investigated by evaluating the remaining Nluc activity after 20 min incubation at specific temperatures. As shown in Fig. 3B, ELP-D-Nluc-BAP retained approximately 80% of its luminescence activity after incubation at 60 °C, relative to the activity after incubation at 4 °C. Above 70 °C, the activity rapidly decreased. These results suggest that the Nluc activity of ELP-D-Nluc-BAP was retained even after incubation at the transition temperature required for preparation of nanoparticles.

Formation of thermoresponsive ELP-D-Nluc-BAP protein nanoparticles

To determine whether ELP-D-Nluc-BAP could form nanoparticles, the thermal transition properties of both ELP-D and ELP-D-Nluc-BAP were evaluated by monitoring the optical density at 350 nm as the aqueous solutions were heated from 20 to 50 °C, and subsequently cooled. During heating, thermal transitions of ELP-D and ELP-D-Nluc-BAP occurred around 34.5 and 37.5 °C, respectively (Fig. 4A). Upon cooling from 50 to 20 °C, a thermal transition was observed for ELP-D, but not for ELP-D-Nluc-BAP. Rincon *et al.* reported that poly(VPAVG) forms stable microparticles above a transition temperature, and that the aggregated forms are retained even after cooling.[33] However, a previous study from our lab showed that $(PAVGV)_{42}$-D_{44} nanoparticles exhibited a slight thermal transition upon cooling. Taken together, these results suggest that

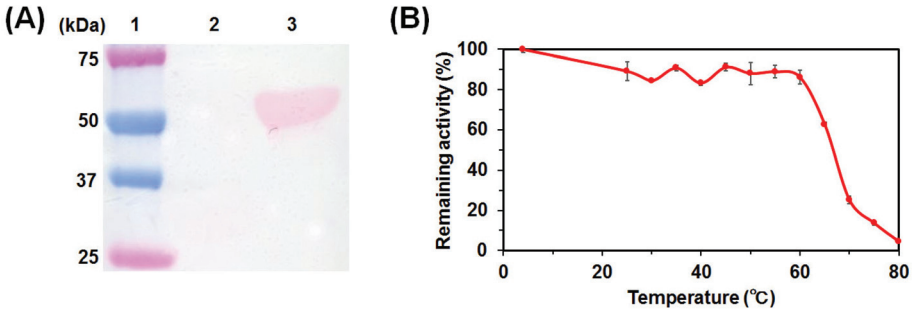

Fig. 3 Characterization of the Nluc and BAP moiety of the fusion protein. (a) Western-blot analysis of ELP-D and ELP-D-Nluc-BAP proteins. The signal was detected with streptavidin-alkaline phosphatase (ALP). Lane 1: molecular weight marker; lane 2: ELP-D; lane 3: ELP-D-Nluc-BAP. (b) Remaining luciferase activity of ELP-D-Nluc-BAP protein after 20 min incubation at individual temperature. The activity at 4 °C incubation of the protein was set as 100%. The absolute 100% value of ELP-D-Nluc-BAP was 6.1×10^6 RLU per s.

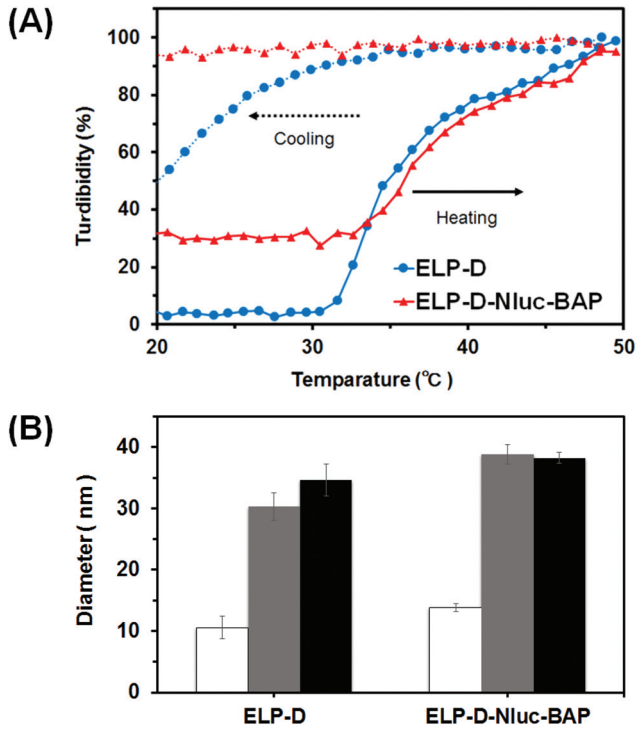

Fig. 4 Thermoresponsive nanoparticle formation. (A) Turbidity profile of ELP-D (●) and ELP-D-Nluc-BAP (▲). The turbidity profiles of polypeptides were obtained by monitoring the optical density at 350 nm. (B) Hydrodynamic size distribution of the formed nanoparticles was measured by dynamic light scattering (DLS) at 20 °C (white bar), 37 °C (gray bar) and 20 °C, cooled after incubation at 37 °C (black bar).

displaying Nluc on the surface of nanoparticles prevented the nanoparticles from collapsing.

Our designed fusion protein was expected to form nanoparticles following incubation at the transition temperature due to the presence of poly-aspartic acid chains. The particle sizes were evaluated by DLS. The size distributions were first measured at 20 °C, and found to be around 10 and 14 nm for ELP-D and ELP-D-Nluc-BAP, respectively, suggesting that the proteins existed predominantly as monomers below the transition temperature. Above the transition temperature (at 45 °C), the diameters of ELP-D and ELP-D-Nluc-BAP were increased to around 30 and 40 nm, respectively (Fig. 4B), indicating the formation of nanoparticles. As mentioned above, the sizes of the resulting nanoparticles were likely regulated by the charged repulsion of the poly-aspartic acid chains. After cooling to 20 °C, the particle sizes of ELP-D and ELP-D-Nluc-BAP were maintained at around 30 nm and 40 nm, respectively, demonstrating that ELP-D and the designed ELP-D-Nluc-BAP fusion protein form stable nanoparticles after heating above the transition temperature.

Nanoparticle-based enhanced ELISA

Here, ELISA was performed using Nluc-displaying nanoparticles as detector probes. AFP was selected as the test analyte because of its importance as a biomarker for liver, lung, breast, and rectal cancers, and the need to develop accurate and sensitive methods that allow for early cancer diagnosis.[34] Various concentrations of AFP were analyzed by ELISA, using ELP-D-Nluc-BAP nanoparticles and monomeric ELP-D-Nluc-BAP (Fig. 5). Instead of AFP, human serum albumin (HSA) was used as a negative control. In the negative control experiment, an ELP-D-Nluc-BAP nanoparticle was used as a detector probe. The signal of control was increased gradually depend on the concentration of HSA. It would be caused by nonspecific binding of HSA. Compared to the negative control, experiments with AFP showed a remarkably increasing signal. A standard curve was measured by the enhanced ELISA technique using AFP standards over a concentration range of 1–500 pg mL^{-1}. The results showed that the LOD of AFP using ELP-D-Nluc-BAP nanoparticles was 25.9 pg mL^{-1}, and that the system could still detect and allow clear discrimination between the analyte of interest and the negative control. In contrast, the LOD of AFP using monomeric ELP-D-Nluc-BAP as the detection probe in the ELISA was 248.1 pg mL^{-1}. Thus, the sensitivity of the enhanced ELISA using ELP-D-Nluc-BAP nanoparticles was 10 times higher than ELISA using monomeric ELP-D-Nluc-BAP, and is most likely due to the higher amount of Nluc molecules displayed on the surfaces of the nanoparticles compared with the monomeric protein. The level of Nluc activity enhancement in ELISA was not higher than our

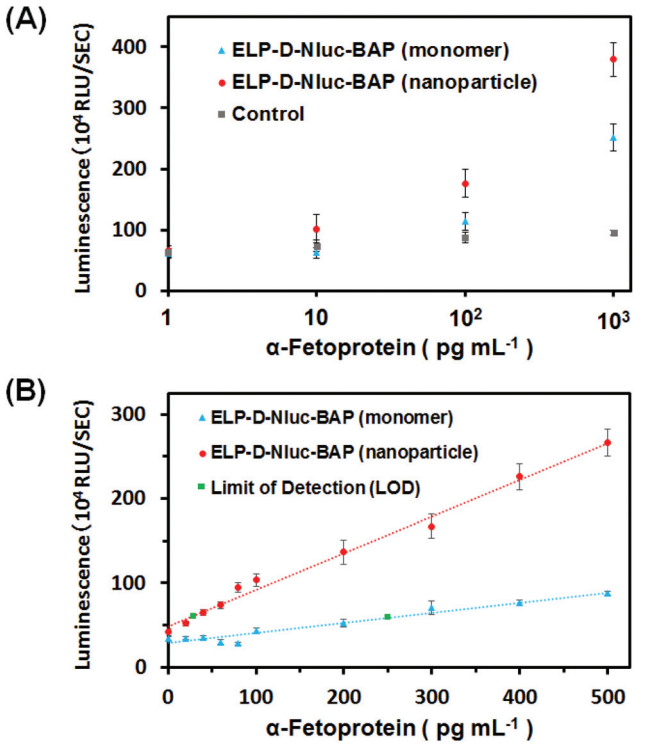

Fig. 5 Dose–response curves for AFP detection using a nanoparticle-based probe and a monomer version probe. The concentration of AFP ranged from 1 pg mL^{-1} to 100 pg mL^{-1} exponentially (A) and from 0 pg mL^{-1} to 500 pg mL^{-1} proportionally (B). Each value presents the mean from 3 replicates (n = 3).

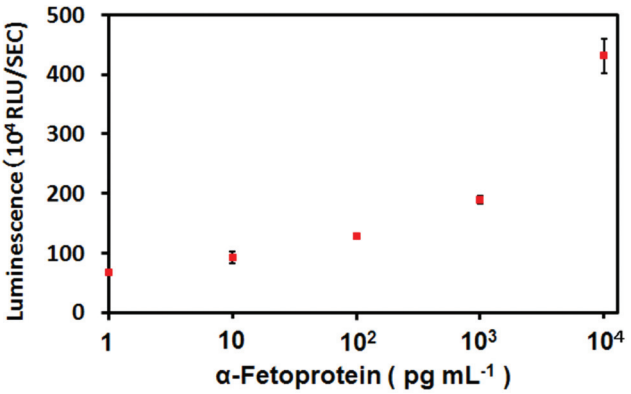

Fig. 6 Standard curves of AFP in human serum constructed by nanoparticle-based enhanced ELISA. Each value presents the mean from 3 replicates (n = 3).

expectation. It would be caused by steric hindrance or electrostatic repulsion between each nanoparticle and thereby it was not able to form complexes between antibodies and nanoparticles.

Finally, we performed nanoparticle-based enhanced ELISA to demonstrate the detection of AFP in human blood serum. Tumor markers (*e.g.*, proteins) can often be found in the blood or urine when cancer is present. Therefore, it is important to be able to detect their presence in biological samples. Fig. 6 shows a signal increase as the concentration of AFP in the testing buffer was increased from 10 pg mL^{-1} to 10 000 pg mL^{-1}. From this result it was clear that ELP-D nanoparticle probe-based ELISA can be applied for the detection of samples in serum. It is important to note that these results can be achieved by the simple introduction of ELPs as multi-enzyme carriers within well-established ELISA procedures, with no significant changes in the experimental protocols. For this reason, the enhanced ELISA technology developed herein can be easily extended to other important ELISA tests (*e.g.*, diagnosis).

Conclusions

Luciferase-displaying protein nanoparticles were genetically designed for use as highly sensitive detection probes. A fusion protein comprised of ELP with a poly-aspartic acid chain, NanoLuc® luciferase, and a biotin acceptor peptide was genetically constructed. The fusion protein self-assembled upon incubation above the transition temperature and formed stable nanoparticles due to the inherent ELP sequence and charged repulsion resulting from the presence of poly-aspartic acid chains. The detection sensitivity for the cancer marker AFP was found to be about 10 times higher using ELP-D-Nluc-BAP nanoparticle-based ELISA, compared to the assay using the monomer form of the protein. Taken together, multivalent display of luciferases on the nanoparticle surfaces results in improvements in detection sensitivity and may open the possibility of incorporating this system into advanced biosensors in the future.

Acknowledgements

This work was supported in part by Japan Society for the Promotion of Science (JSPS).

Notes and references

1 C. P. Jia, X. Q. Zhong, B. Hua, M. Y. Liu, F. X. Jing, X. H. Lou, S. H. Yao, J. Q. Xiang, Q. H. Jin and J. L. Zhao, *Biosens. Bioelectron.*, 2009, **24**, 2836.
2 P. D. Wagner and M. Verma, *Ann. N. Y. Acad. Sci.*, 2004, **1022**, 9.
3 D. S. Wilson and S. Nock, *Angew. Chem., Int. Ed.*, 2003, **42**, 494.
4 E. V. Stevens, L. A. Liotta and E. C. Kohn, *Int. J. Gynecol. Cancer*, 2003, **13**, 133.
5 Y. Zhao, D. Du and Y. Lin, *Biosens. Bioelectron.*, 2015, **72**, 348.
6 D. Du, L. Wang, Y. Shao, J. Wang, M. H. Engelhard and Y. Lin, *Anal. Chem.*, 2011, **83**, 746.
7 A. Ambrosi, F. Airò and A. Merkoçi, *Anal. Chem.*, 2010, **82**, 1151.
8 G. Lai, F. Yan, J. Wu, C. Leng and H. Ju, *Anal. Chem.*, 2011, **83**, 2726.
9 T. Jiang, Y. Song, T. Wei, H. Li, D. Du, M. J. Zhu and Y. Lin, *Biosens. Bioelectron.*, 2016, **77**, 687.
10 S. Bi, Y. Yan, X. Yang and S. Zhang, *Chemistry*, 2009, **15**, 4704.
11 L. Chen, C. Chen, R. Li, Y. Li and S. Liu, *Chem. Commun.*, 2009, 2670.
12 H. Wang, J. Wang, C. Timchalk and Y. Lin, *Anal. Chem.*, 2008, **80**, 8477.
13 X. Yu, B. Munge, V. Patel, G. Jensen, A. Bhirde, J. D. Gong, S. N. Kim, J. Gillespie, J. S. Gutkind, F. Papadimitrakopoulos and J. F. Rusling, *J. Am. Chem. Soc.*, 2006, **128**, 11199.
14 R. Malhotra, V. Patel, J. P. Vaqué, J. S. Gutkind and J. F. Rusling, *Anal. Chem.*, 2010, **82**, 3118.
15 G. Lai, F. Yan and H. Ju, *Anal. Chem.*, 2009, **81**, 9730.
16 D. Du, Z. Zou, Y. Shin, J. Wang, H. Wu, M. H. Engelhard, J. Liu, I. A. Aksay and Y. Lin, *Anal. Chem.*, 2010, **82**, 2989.
17 Y. Song, Y. Luo, C. Zhu, H. Li, D. Du and Y. Lin, *Biosens. Bioelectron.*, 2016, **76**, 195.
18 Y. Yang, A. M. Asiri, Z. Tang, D. Du and Y. Lin, *Mater. Today*, 2013, **16**, 365.
19 W. Cai, I. R. Gentle, G. Q. Lu, J. J. Zhu and A. Yu, *Anal. Chem.*, 2008, **80**, 5401.
20 L. Yuan, X. Hua, Y. Wu, X. Pan and S. Liu, *Anal. Chem.*, 2008, **80**, 5401.
21 H. Xu, D. Wang, S. He, J. Li, B. Feng, P. Ma, P. Xu, S. Gao, S. Zhang, Q. Liu, J. Lu, S. Song and S. Fan, *Biosens. Bioelectron.*, 2013, **50**, 251.
22 X. Yu, B. Munge, V. Patel, G. Jensen, A. Bhirde, J. D. Gong, S. N. Kim, J. Gillespie, J. S. Gutkind, F. Papadimitrakopoulos and J. F. Rusling, *J. Am. Chem. Soc.*, 2006, **128**, 11199.

23 Y. Wu, C. Chen and S. Liu, *Anal. Chem.*, 2009, **81**, 1600.
24 D. E. Meyer, K. Trabbic-Carlson and A. Chilkoti, *Biotechnol. Prog.*, 2001, **17**, 720.
25 D. E. Meyer and A. Chilkoti, *Nat. Biotechnol.*, 1999, **17**, 1112.
26 Y. Fujita, M. Mie and E. Kobatake, *Biomaterials*, 2009, **30**, 3450.
27 R. Matsumoto, R. Hara, T. Andou, M. Mie and E. Kobatake, *J. Biomed. Mater. Res., Part B*, 2014, **102**, 1792.
28 Y. Assal, Y. Mizuguchi, M. Mie and E. Kobatake, *Bioconjugate Chem.*, 2015, **26**, 1672.
29 M. P. Hall, J. Unch, B. F. Binkowski, M. P. Valley, B. L. Butler, M. G. Wood, P. Otto, K. Zimmerman, G. Vidugiris, T. Machleidt, M. B. Robers, H. A. Benink, C. T. Eggers, M. R. Slater, P. L. Meisenheimer, D. H. Klaubert, F. Fan, L. P. Encell and K. V. Wood, *ACS Chem. Biol.*, 2012, **7**, 1848.
30 J. E. Cronan, *J. Biol. Chem.*, 1990, **265**, 10327.
31 P. J. Schatz, *Nat. Biotechnol.*, 1993, **11**, 1138.
32 D. T. McPherson, J. Xu and D. W. Urry, *Protein Expression Purif.*, 1996, **7**, 51.
33 A. C. Rincon, I. T. Molina-Martinez, B. de Las Heras, M. Alonso, C. Bailez, J. C. Rodriguez-Cabello and R. Herrero-Vanrell, *J. Biomed. Mater. Res.*, 2006, **78**, 343.
34 D. Badera, A. Riskina, O. Vafsia, A. Tamir, B. Peskin, N. Israel, R. Merksamer, H. Dar and M. David, *Clin. Chim. Acta*, 2004, **349**, 15.